Triggering Standard Model Higgs processes in the ATLAS experiment

V. Perez-Reale on behalf of the ATLAS TDAQ*) and Higgs WG

Laboratory for High Energy Physics, University of Bern, Switzerland

Received 1 September 2004;
final version 15 September 2004

The search for the Higgs boson is a major physics goal of the future Large Hadron Collider. The potential to trigger on Standard Model Higgs boson with electrons or photons in the final state has been studied for the low mass range $m_H < 2m_Z$ for the ATLAS experiment at the LHC. Analyses for the $H \to ZZ^*$, $H \to \gamma\gamma$ and $H \to WW^*$ decay modes have been studied using a realistic simulation of the expected detector performance for both the start–up and the design luminosity scenarios. The results obtained demonstrate that the ATLAS trigger is efficiently selecting Higgs candidates for these discovery channels.

PACS: 62.20
Key words: Higgs, trigger, efficiencies

1 Introduction

The search for the Higgs boson is one of the major goals of the ATLAS experiment at the Large Hadron Collider (LHC). The LHC is designed to collide protons at a center of mass energy of 14 TeV with a bunch crossing rate of 40 MHz. ATLAS is a multipurpose detector designed to have a 4π hermiticity around the interaction point. The detector includes a central Inner Tracker surrounded by a 2T solenoid, Electromagnetic and Hadronic Calorimeters outside the solenoid and in the forward regions, and an air-core toroid Muon Spectometer.

Many studies have established that a Standard Model (SM) Higgs Boson can be discovered with high significance over the full mass range of interest, from the lower limit set by the LEP experiments of 114.1 GeV [1] up to about 1 TeV [2]. At the LHC, the SM Higgs boson production cross-section has contributions from various subprocesses, of which gluon-gluon fusion and vector boson fusion radiated from initial–state quarks are the most important ones. The feynmann diagrams for these two processes are shown in Fig 1. The relative contributions of the two processes depend on the Higgs boson mass.

The SM Higgs boson is searched for at the LHC in various decay channels, the choice of which is given by the signal rates and the signal–to–background ratios in the various mass regions. For the low mass region, $m_H < 2m_Z$, a combined 5σ[1]) significance can be reached with the ATLAS detector by combining the decays $ttH \to tt b\bar{b}$, $H \to \gamma\gamma$, $H \to ZZ^*$, and $H \to WW^*$ decay via Vector Boson Fusion

*) The HLT/DAQ/Controls TDR [2].

[1]) σ is defined as $S/\sqrt{B}$ where S is the number of signal events and B the number of background events

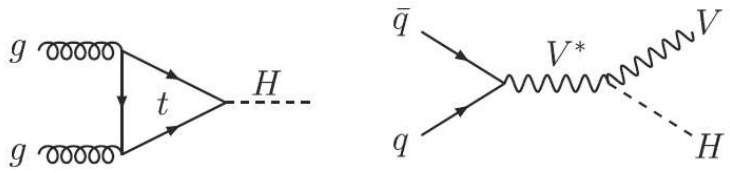

Fig. 1. Standard Model Higgs Processes.

(VBF) [3]. This significance is for an integrated luminosity of 10 fb^{-1}, corresponding to data collected in approximately one year of data taking at the initial LHC luminosity ($2 \times 10^{33}\ cm^{-2}s^{-1}$).

The ATLAS experiment will face the challenge of efficiently selecting interesting Higgs candidate events in proton-proton collisions at 14 TeV center of mass energy, whilst rejecting an enormous number of background events. The online trigger selection will reduce the initial event rate of around 10^9 Hz to 200 Hz going to mass storage [4]. At the LHC the difficulty to extract the Higgs signal from the huge QCD background dictates the choice of channels with leptons and photons. For the low mass region, $m_H < 2m_Z$, the following Higgs decay channels include lepton and gammas in the final state: $H \to \gamma\gamma$, $H \to ZZ^* \to 4l$, and $H \to WW^* \to l\nu l\nu$ decay via VBF.

A large part of the physics programme will rely heavily on lepton and photon triggers. Given the required large selectivity of the ATLAS trigger O(10^{-7}) due to the rare nature of some of the Higgs signatures at the LHC collider, it is essential to understand the trigger efficiencies and the background rate of Higgs processes at each step of the event selection.

In the present study, the analyses of the leptonic and photon Higgs decay modes in the low mass region have been performed using realistic simulations of the expected performance of the ATLAS detector and pile–up [5]. We present the trigger performance for these channels at start–up LHC luminosity ($2 \times 10^{33}\ cm^{-2}s^{-1}$) and at design luminosity ($1 \times 10^{34}\ cm^{-2}s^{-1}$).

In Section 2, the event generation for the signal processes are discussed. Important experimental issues of the trigger selection and leptonic and gamma selection of these processes are addressed in Section 3. General signal selection criteria are presented in Section 4, and a detailed analysis of the Higgs channels $H \to \gamma\gamma$, $H \to ZZ^* \to 4l$, $H \to WW^* \to l\nu l\nu$ decay via VBF are considered in Sections 5, 6 and 7.

2 Signals

The following Higgs boson decay modes have been considered in this analyses:

- $H \to \gamma\gamma$
- $H \to ZZ^* \to 4e$
- $H \to ZZ^* \to 2e2\mu$
- $H \to WW^* \to e\nu e\nu$ via VBF

All final states consist of at least one high p_T lepton or gamma.

The signal processes have been generated using PYTHIA 6.2 Monte Carlo event generator [6]. Initial–and final–state radiation have been switched on.

GEANT3 [7], the package for the full simulation of the ATLAS detector, has been used to perform the detector simulation for all processes considered. Pile–up was simulated by adding in average to these processes for the low (design) luminosity (4.6) 23 minimum bias events per bunch crossing in order to simulate the real LHC conditions. The effect due to electronic noise has been simulated as well.

To study the electron and photon trigger efficiencies fully simulated single electrons with transverse energy $E_T = 25(30)\ GeV$ and single photons with $E_T =$ 20(60) GeV have been used at low (design) luminosity. To evaluate the trigger rates for these thresholds, around ten million fully simulated QCD dijet events were used. In addition, physics events such as $Z \to ee$ adn $W \to e\nu$ have been added. The events were generated with PYTHIA and on the parton level each jet was required to have a p_T of at least 17(25) GeV at low (design) luminosity. Events which would not pass the first level trigger are immediatly rejected before being processed by GEANT3 by applying a particle level filter before full simulation.

3 Experimental Issues

In this section, several experimental issues that are common to all Higgs studies are discussed. Among them are the trigger online selection and the electron/gamma selection.

3.1 Trigger Selection

The ATLAS trigger system must accept the high 40 MHz bunch crossing frequency and reduce it to a manageable rate of O(200 Hz). The online selection is based on a three level hierarchy. The first level trigger (L1) will reduce the initial event rate of 10^9 Hz to O(100 kHz). The High–Level Triggers (HLT), which are comprised of the second level (L2) and Event Filter (EF), must reduce the rate further to O(200 Hz) going to mass storage [8].

The hardware based L1 Trigger selection is based on high p_T signals coming from the calorimeter and muon detectors. The HLT selection is software based and has access to full granularity information from the calorimeter and inner detector. The L2 trigger is guided by the geometrical information provided by the L1 result. Only the data in the region identified by L1 are examined. The EF has access

Table 1. Trigger Menus, showing the inclusive trigger for Higgs processes including leptonic and gamma decays for low and design luminosity. The trigger item e25i refers to the requirement that within the event at least one electron with an E_T of at least 25 GeV is efficiently selected, i stands for this object fulfilling isolation criteria.

Object	Low luminosity	Design luminosity	Higgs Coverage
electrons	$e25i, 2e15i$	$e30i, 2e20i$	$H \to WW^*/ZZ^*$
photons	$\gamma 60i, 2\gamma 20i$	$\gamma 60i, 2\gamma 20i$	$H \to \gamma\gamma$
muons	$\mu 20i, 2\mu 10$	$\mu 20i, 2\mu 10$	$H \to WW^*/ZZ^*$
electrons + muons	$\mu 10 + e15i$	$\mu 10 + e20i$	$H \to WW^*/ZZ^*$

to the full event reconstruction or to a reconstruction guided by the result of L2. Only events surviving this three-stage triggering system can be part of subsequent physics analysis.

To guarantee optimal acceptance to new physics, the ATLAS online selection is presently based on an inclusive selection criteria, such as high p_T single and double object triggers. A large part of the physics programme will rely heavily on the inclusive single and dilepton triggers, involving electrons and muons for Higgs boson searches.

Table 1 shows the trigger menus for the electron/gamma triggers. For each trigger menu item the SM Higgs decay channels with electron and gammas in the final state are shown for the low and design luminosity scenarios. In addition the table shows with which trigger menu item we want to select the various Higgs decay channels in the low mass region. The energy thresholds of the trigger menus indicate the transverse energy value above which the selection has good efficiency for true objects of the specified type. For example, the inclusive single and di–photon triggers will possibly select a light Higgs boson via its decay $H \to \gamma\gamma$ in case $m_H < 150$ GeV.

All channels considered in this study have electrons or gammas in the final state and should be triggered by at least one of the trigger menu items for electron or photon objects. The ATLAS trigger acceptance covers the pseudo–rapidity region $|\eta| < 2.5$ for electrons and photons.

3.2 Electron/gamma Identification

The procedure for the selection of electron and photon candidates is as follows:

– At L1 electromagnetic (EM) clusters are selected based on the calorimeter information. The transverse energy of the EM object must exceed a certain threshold value. Isolation around the cluster and isolation in the hadronic calorimeters are also required.

– The L2 uses the information and the direction of the EM clusters selected by the L1 trigger and only the regions around these clusters are further analyzed. The L2 selection for electrons and photons first analyzes the shower shapes in the EM calorimeter and the energy leakage in the hadronic calorimeter. If a candidate is consistent with an electron it is further processed and in the next step tracks are searched for in the inner detector and the cluster and track quantities are compared. For photons tighter shower shape cuts are applied.

– In case the trigger menus are fulfilled the event is passed to the EF. At this level the information of the complete event is available and either the L2 result can be used as a seed to start the reconstruction from a region of interest identified by L1 or the whole event can be analysed. Compared to L2 more precise alignment and calibrations are available in the EF. Similar to L2, electrons and photons at the EF are selected using calorimeter and inner detector information. In the case of electrons, bremsstrahlung recovery has been performed.

4 Electron/gamma Trigger Efficiencies

In the Higgs event selection, the electron–gamma selection applied has been optimized using single electrons and photons.

Using Monte Carlo simulations the performance of the electron/gamma triggers has been evaluated in terms of the efficiency for the signal channels and the rate expected for the selection of the L1, L2 calorimeter and EF trigger.

The online trigger levels are set up to select efficiently isolated electrons with a transverse energy (E_T) of at least 25 GeV at start-up luminosity. Table 2 shows the electron efficiencies and expected rates for the single and double electron trigger after each trigger step factorized by detector: calorimeter (L2Calo, EFCalo), inner detector (EFID) and combined calorimeter–inner detector (EFIDCalo). For an overall $76.2 \pm 0.4\%$ electron efficiency a rate of 46 ± 4 Hz has been found. This final rate is composed of 50% of clusters coming from 'real' electrons, (electrons from b and c decays and conversions). An efficiency of $57.3 \pm 1.5\%$ is found for the double electron trigger at low luminosity corresponding to a rate of a few Hz [9].

The single photon trigger gives an efficiency of 80% after each trigger step for low luminosity, corresponding to 1.5 Hz rate. The efficiency to select two isolated photons was found to be 64% corresponding to a rate of 8 ± 3 Hz.

5 The $H \to ZZ^* \to 4l$ decay mode

The trigger efficiencies for various Higgs process shown in Table 3 were calculated for lepton and gamma decays in a geometrical acceptance region of $|\eta| < 2.5$ (region of precision physics)[2]). In the present study the efficiency to trigger on a SM Higgs process is defined in two ways. The Trigger Efficiency is defined as the

[2]) As has been done in previous ATLAS studies [2]

Table 2. Trigger efficiencies and rates for the single electron trigger $e25i$ and double electron trigger $2e15i$ at low luminosity. The trigger selection at each level is factorized by detector: calorimeter, inner detector, combined calorimeter–inner detector.

	$e25i$		$2e15i$	
Trigger Selection	Trigger Efficiency (%)	Rates	Trigger Efficiency (%)	Rates
L1	95.5 ± 0.2	8.6 kHz	94.4 ± 0.5	3.5 kHz
L2Calo	92.9 ± 0.3	1.9 kHz	82.6 ± 0.9	159 Hz
EFCalo	90.0 ± 0.4	1.1 kHz	81.2 ± 1.0	110 Hz
EFID	81.9 ± 0.2	108 Hz	69.2 ± 1.0	5.6 Hz
EFIDCalo	76.2 ± 0.4	46 Hz	57.3 ± 1.5	1.9 Hz

number of events accepted in a geometrical region in η and with certain transverse momentum. The Overall Trigger Efficiency is normalized respect to events accepted in the whole phase space region.

The decay channel $H \to ZZ^* \to 4l$ provides a rather clean signature in the low mass range for Higgs searches at the LHC. In addition to the irreducible background from ZZ^* and $Z\gamma^*$ continuum production, there are large reducible backgrounds from $t\bar{t}$ and $Zb\bar{b}$ production. In this section, the trigger efficiencies for the $H \to ZZ^* \to 4l$ channel are presented. The following event topologies have been considered with both electrons and muons in the final state: $4e$ and $2e2\mu$.

5.1 $H \to ZZ^* \to 4e$

In addition to the electron identification criteria described in section 3, the following kinematical cuts were applied at Monte Carlo level to the reconstructed events: two electrons with $p_T > 20$ GeV and $|\eta| < 2.5$ and two additional electrons with transverse momentum $p_T > 7$ GeV and $|\eta| < 2.5$ are required.

The trigger efficiency for a Higgs with $m_H = 130$ GeV is shown in Table 3 for low and design luminosity scenarios. The trigger efficiency as well as the efficiency per trigger menu item are given. For the low luminosity scenario the trigger is found to select 96.7% of these Higgs events fulfilling the kinematic cuts specified above. The overall trigger efficiency for this scenario is 45.8%. The trigger efficiency for the design luminosity case is 95.5%. The trigger efficiency is very high because only one or two electrons are required at trigger level while four electrons are present in the event for this process.

The dependency of the trigger efficiency for a given Higgs process on the Higgs mass was also studied. Figure 2 shows the trigger efficiency as a function of the Higgs mass for low and design luminosity. The trigger efficiency increases slightly with the Higgs mass. This is expected since for larger Higgs masses the electrons

Table 3. Trigger Efficiencies with respect to kinematical cuts described in text for Higgs channels: $H \to 4e$ (130 GeV), $H \to 2e2\mu$ (130 GeV), $H \to e\nu e\nu$ (170 GeV) and $H \to \gamma\gamma$ (120 GeV) at low luminosity and at design luminosity.

Trigger	Luminosity	$H \to 4e$	$H \to 2e2\mu$	$H \to e\nu e\nu$	$H \to \gamma\gamma$
$e25i$	*low*	96.5 ± 0.2	76.2 ± 0.4	89.1 ± 1.2	
$2e15i$	*low*	95.8 ± 0.2	63.7 ± 0.5	84.4 ± 1.4	
$e25i$ *or* $2e15i$	*low*	96.7 ± 0.2	76.9 ± 0.4	89.5 ± 1.2	
$e30i$	*design*	96.0 ± 0.4	70.1 ± 0.5		
$2e20i$	*design*	94.5 ± 0.4	59.4 ± 0.5		
$e30i$ *or* $2e20i$	*design*	95.5 ± 0.3	71.0 ± 0.5		
$\gamma 60i$	*low*				57.0 ± 0.7
$2\gamma 20i$	*low*				74.0 ± 0.6
$\gamma 60i$ *or* $2\gamma 20i$	*low*				83.0 ± 0.5

of the decay are more energetic and well above the trigger threshold.

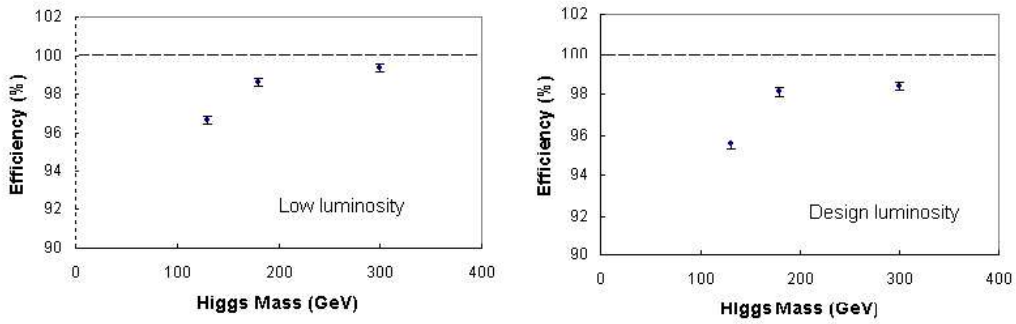

Fig. 2. Trigger Efficiency as a function of the Higgs mass for the Higgs channel $H \to ZZ^* \to 4e$ for low and design luminosity.

Dedicated studies have shown that less than 1% of the Higgs events that would fulfill the offline analyses criteria are rejected by the online selection presented here. The loss of events is mainly due to the fact that the L1 trigger selection is hardware based having only coarse granularity calorimeter information available. This

results in a poorer energy resolution compared to the offline selection. Other factors involved is the fact that the offline and online use different electron identification selection strategies and are using different energy calibrations.

5.2 $H \to ZZ^* \to 2e2\mu$

The electron identification criteria described in section 3 for this process is proceeded by the following kinematical cuts at MC level after event reconstruction: two leptons with $p_T > 20$ GeV and $|\eta| < 2.5$ and two additional leptons with transverse momentum $p_T > 7$ GeV and $|\eta| < 2.5$ are required. Figure 3 shows an event display of a Higgs event with this decay in a ρZ projection in barrel and endcap calorimeters of the ATLAS detector.

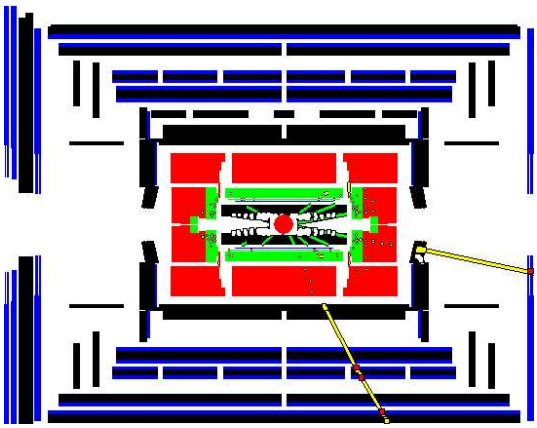

Fig. 3. Event display of the Higgs process $H \to ZZ^* \to 2e2\mu$. ρZ projection in barrel and endcap calorimeters of the ATLAS detector.

The trigger efficiency for a Higgs mass of 130 GeV for the single and double object electron trigger menu is shown in Table 3 for low and design luminosity scenarios. For the low luminosity scenario the trigger is found to be 76.9% efficient selecting electrons. The overall trigger efficiency for this scenario is 29.9%. The trigger efficiency for the high luminosity scenario is 71.0%.

Furthermore, if the muon and electron plus muon trigger menus are included in the analyses the trigger efficiencies for this process will increase by at least 20%. Further studies will be performed.

6 The $H \to \gamma\gamma$ decay mode

The $H \to \gamma\gamma$ is a promising channel for Higgs searches in the mass range 100 GeV $< m_H <$ 150 GeV, where the production cross-section and the decay branching ratio are both relatively large.

This decay places severe requirements on the performance of the electromagnetic calorimeter. Excellent energy and angular resolution are needed to observe the narrow mass peak above the irreducible prompt $\gamma\gamma$ continuum. Powerful gamma identification capability is required to reject the large QCD reducible background in which one or two jets are misidentified as gammas. The fine granularity of the first sampling of the electromagnetic calorimeter offers the possibility to separate gammas from hadrons. A track veto and the reconstruction with gamma conversions will help further reduce the backgrounds.

In the analyses of this channel the following kinematical cuts at MC level were applied to the selection of events: one photon with $p_T > 40$ GeV and $|\eta| < 2.4$ and an additional photon with transverse momentum $p_T > 25$ GeV and $|\eta| < 2.4$ and gammas in the barrel–endcap transition region $1.37 < |\eta| < 1.52$ are excluded.

The trigger efficiency for a Higgs mass of 120 GeV for the single and double object photon trigger menu is shown in Table 2 for low luminosity scenario. The trigger is found to be 83.0% efficient for this Higgs decay mode. The overall trigger efficiency for this scenario is 46%. The trigger efficiency in the η acceptance region is found to be consistent with previous studies [10].

7 The VBF $H \to WW^* \to e\nu e\nu$ decay mode

For $m_H < 2m_Z$, vector boson fusion amounts in leading order to about 20% of the total Higgs production cross–section and becomes more important with increasing mass. Studies in the ATLAS collaboration have demonstrated that the ATLAS experiment has a large discovery potential in the $H \to WW^* \to l^+l^- P_T^{miss}$ channel [11].

The dominant backgrounds for this process are $t\bar{t}$ production where the W bosons from the top decays leptonically, and Electroweak W pair production.

The final state associated with events from these leptonic decay process include the two quark jets from the hard scattering in conjunction with two leptons and missing p_T from the decay of the W bosons. In this analysis two different kinematical cuts at MC level were applied to the leptonic selection of the reconstructed events. The first selection required two leptons with $p_T > 7$ GeV and $|\eta| < 2.5$. The second selection required that these leptons are electrons with $p_T > 15$ GeV and $|\eta| < 2.5$.

The trigger efficiencies for a Higgs Boson with a mass of 170 GeV are given in Table 3 for low luminosity. In this study only the L1 and EF trigger is considered compared to the Higgs analyses discussed in the previous sections. The results should not differ considerably when the L2 trigger is applied since the L2 selection is set–up in such a way to not reject events prematurely. In the case were two electrons are required at the MC level the trigger efficiency is 89.5%.

8 Conclusions

The trigger efficiencies for the Standard Model Higgs boson in the mass range below 190 GeV has been studied for several electron and gamma decay modes. It

has been demonstrated that the ATLAS online selection is efficient for selecting events for the Higgs channels with electron and photon decays: $H \to ZZ^* \to 4e$, $H \to ZZ^* \to 2e2\mu$, $H \to \gamma\gamma$ and $H \to WW^* \to e\nu e\nu$ via VBF.

In addition, the results obtained demonstrate that the trigger menus for electrons and photons are well adapted for the Higgs physics programme envisaged at LHC. The overlap in the thresholds for transverse energy of the single and double object trigger makes the trigger selection very robust and stable. Furthermore the study of the $H \to ZZ^* \to 4e$ channel has proven that the trigger online selection does not reject events prematurely.

The present study confirms that the present inclusive trigger selection is as well efficient for more challenging channels that involve other signatures apart from leptons and photons such as missing transverse energy for the $H \to WW^* \to e\nu e\nu$ via VBF channel.

This work has been performed within the ATLAS collaboration, and we thank collaboration members for helpful discussions. We have made use of reconstruction software and analysis tools which are result of collaboration wide efforts.

References

[1] LEP Collaborations: CERN–EP/2001–55, hep-ex/0107029 (2001).

[2] ATLAS Collaboration: Detector and Physics Performance, CERN/LHCC/99-14 (1999).

[3] S. Gentile: Search for Higgs Bosons with the ATLAS detector, CERN, ATL–PHYS–2004-009 (2004).

[4] ATLAS Collaboration: ATLAS High–Level Trigger and Data Aquisition and Controls, Techincal Design Report, CERN/LHCC/2003-022 (2003).

[5] ATLAS Data Challenge 1 Task Force: A Step Towards A Computing Grid For The LHC Experiments : ATLAS DC1, CERN, CERN–PH–EP–2004–028 (2004).

[6] PYTHIA 6.206 manual: LU TP 01-21, hep-ph/0108264.

[7] R. Brun et al.: GEANT3 Detector Description and Simulation Tool, CERN DD/EE/84-1 (1986).

[8] M. Grothe et al.: Architecture of the ATLAS High Level Trigger Event Selection Software, CERN, ATL–DAQ–2003–030(2003).

[9] J. Baines et al.: Performance Studies of the High Level Electron Trigger, CERN, ATL–COM–DAQ–2003–020 (2003).

[10] M. Wielers: Photon Identification with the ATLAS detector, CERN, ATL–PHYS–99–016 (1999).

[11] S. Asai et al.: Prospects for the Search for a Santandard Model Higgs Boson in ATLAS using Vector Boson Fusion, ATLAS Scientific Note SN–ATLAS–2003–024, hep-ph/0402254 (2003).